Volume 6, Issue 3, 2016, 1280-1287 **ISSN 2069-5837**

Biointerface Research in Applied Chemistry

www.BiointerfaceResearch.com

Original Research Article **Open Access Journal**

Received: 21.03.2016 / Revised: 16.04.2016 / Accepted: 18.05.2016 / Published on-line: 15.06.2016

Characterization of iron nanoparticles produced with green tea extract: a promising material for nitric oxide delivery

Bruna Santiago de Oliveira Silva[1], Amedea Barozzi Seabra[1,2*]

[1]Exact and Earth Sciences Departament, Universidade Federal de São Paulo, Diadema, SP, Brazil.
[2]Center of Natural and Human Sciences, Universidade Federal doABC, Santo André, SP, Brazil

*corresponding author e-mail address:***amedea.seabra@gmail.com**

ABSTRACT

Iron nanoparticles were synthesized by green tea extract and used as nitric oxide (NO) donor. The nanoparticles were obtained by the reduction of Fe^{2+}, Fe^{3+}, or a mixture of Fe^{2+}/Fe^{3+} by green tea extract, at room temperature within few minutes. The as-synthesized iron nanoparticles were characterized by X-ray diffraction, transmission electron microscopy with electron energy loss spectroscopy, scanning electron microscopy with energy dispersive X-ray fluorescence spectrometry, Fourier transform infrared spectroscopy, dynamic light scattering, and ultraviolet-visible spectroscopy. The results showed the formation of iron nanoparticles with average hydrodynamic size of 53.7 ± 10.4 nm, and the presence of polyphenols as capping agents. Free thiol groups on the surface of as-synthesized iron nanoparticles were nitrosated through the addition of an acidified nitrite solution, yielding S-nitroso-iron nanoparticles. The amount of NO covalently bound to the surface of green tea synthesized iron nanoparticles was evaluated by a specific NO electrochemical sensor. The S-nitroso-iron nanoparticles spontaneously released NO in aqueous solution at levels required for biomedical applications. This biogenic iron nanoparticle might find important applications not only in remediation of contaminated soil and water, but also as NO-delivery material able to generate therapeutic amounts of NO in biomedical applications.

Keywords: *Iron nanoparticles, biogenic synthesis, green tea, plant extract, nitric oxide, nitric oxide donor.*

1. INTRODUCTION

Iron based nanoparticles, in particular zero-valent iron nanoparticles (nZVI) have been demonstrated successful environmental applications, including the treatment of contaminated water and soil [1-5]. Indeed, nZVI has been employed for the removal of phosphorous, trihalomethanes from reclaimed-water, polychlorinated aromatic pollutants, metals, as a catalyst for heterogenous Fenton oxidation of amoxicillin, dye discoloration, and the treatment of explosive and nuclear waste [1, 6-11].

Traditional synthesis of iron nanoparticles, including nZVI, is performed by chemical and physical methods [12]. The most employed chemical synthesis method of iron nanoparticles is based on the reduction of Fe^{2+} and/or Fe^{3+} by strong reducing agents, such as sodium borohydride [2, 13]. Chemical routes are based on sol gel technique, thermal decomposition, liquid chemical reduction, gas phase reduction, and chemical vapor condensation [2, 6, 14]. Although chemical synthesis of iron nanoparticles has a higher control over nanoparticle size distribution, this route involves toxic chemicals, yielding hazardous byproducts, contaminating the environment [15, 16]. Moreover, traditional chemical and physical methods are considered expensive due to the high-energy input and manufacturing [16, 17].

To overcome the main limitations of traditional routes to synthesize metallic nanoparticles, biogenic synthesis of nanoparticles has been growing in the last years [16,18-20]. Biogenic routes are considered nontoxic, clean, eco-friendly, and cost effective [15 - 21]. Several biological resources have been employed in biogenic synthesis of metallic nanoparticles, including iron nanoparticles, such as bacteria, algae, fungi, yeast, viruses and plant extracts [7, 15, 16, 20]. In biogenic synthesis of engineered nanoparticles, the experimental conditions are simple, since the reactions occurs at ambient conditions (high energy or high pressure are not required), leading to an energy saving. Moreover, the biological active compound, responsible for the reduction of the metal ion to the metallic nanoparticle, acts as capping agent, reducing the overall cost of the synthesis process [15, 16, 20, 21].

Among the biogenic routes to synthesize metallic nanoparticles, the use of plant extract has gained considerable attention in recent years [15, 16, 22-24]. Indeed, biogenic synthesis of metallic nanoparticles, including iron nanoparticles, by plant extract occurs in a shorter time in comparison to microbe biogenic routes [15]. It is a cost-effective, simple, and eco-friendly route, therefore several reports describe the use of plant extract to synthesize iron nanoparticles. Among them, green tea (*Camellia sinensis*) extract is the most commonly employed plant resource for iron nanoparticle synthesis. For instance, Hoag et al. [3] reported the biogenic synthesis of iron nanoparticles by the reduction of Fe^{3+} by green tea extract at room temperature within a few minutes. Similarly, iron nanoparticles composed mainly by oxide/oxohydrozide were synthesized by green tea extract [25]. Green tea is rich in polyphenols, which act not only as powerful reducing agent but also as a capping agent, stabilizing the obtained nanoparticles [3, 17, 26-28]. In addition, polyphenols are biodegradable and soluble in water [29].

The presence of capping agents on the surface of iron nanoparticles is necessary to minimize particle agglomeration,

since it is known that metallic nanoparticles tend to aggregate due to magnetic forces and van der Waals [13]. During traditional chemical synthesis of iron nanoparticles, the addition of polyelectrolytes or polymers are required to increased steric and/or electrostatic repulsion between the synthesized nanoparticles [12, 30, 31]. In contrast, in plant-mediate synthesis of iron nanoparticles, it not necessary the addition of extra capping agents, since plant polyphenols act as the capping agents. Several studies suggest a core-shell structure for iron nanoparticles, in which the core is composed by zero-valent iron, whereas the shell is composed by mixed valent (Fe^{2+}/Fe^{3+}) oxide due to the oxidation of metallic iron core [1, 6]. In the case of green tea synthesized iron nanoparticles, the presence of polyphenols are expected to stabilize the core/shell iron nanoparticles from further oxidation [6].

In this present work, iron nanoparticles were synthesized by green tea extract and characterized by several techniques. Furthermore, the presence sulfur atoms on the surface of green tea extract synthesized iron nanoparticles was mapped by scanning electron microscopy with energy dispersive X-ray fluorescence spectrometry. The amount of free thiol groups(-SH) on the surface of green tea synthesized iron nanoparticles was titrated with a thiol-specific reagent. The presence of free thiol groups is assumed to be derived from cysteine-containing green tea molecules. These free thiol groups were successfully nitrosated, by the addition of sodium nitrite in slight acidified aqueous solution, leading to the formation of S-nitroso-iron nanoparticles. S-nitroso-moieties act as spontaneous nitric oxide (NO) donor. The free radical NO is involved in the control of several physiological process, such as in the vasodilation, the modulation of immune response, the promotion of wound healing process, the anti-cancer activity, among others [32-34]. Herein, we demonstrated that biogenic synthesized iron nanoparticles act as spontaneous NO donor material.

To our best knowledge, this is the first report to describe the NO release from iron nanoparticles synthesized by green tea extract. Therefore, biogenic synthesized iron nanoparticles can be use not only for environmental applications, but also for carrying and delivering NO in biomedical applications, suggesting the application of this material in fields of environmental remediation and medicine.

2. EXPERIMENTAL SECTION

2.1. Materials.

Green tea powder (*Camellia Sinensis*) (Sumioka Shokuhin Kabushikikaisha, Hiraguti, Japan), iron(III) chloride hexahydrate ($FeCl_3 \cdot 6H_2O$), iron(II) chloride tetrahydrate ($FeCl_2 \cdot 4H_2O$), sodium nitrite ($NaNO_2$), 5`-5-dithiobis(2-nitrobenzoic acid) (DTNB), phosphate-buffered saline (PBS), pH 7.4, ethylenediaminetetraacetic acid (EDTA), copper (II) chloride ($CuCl_2$) (Sigma–Aldrich Ch. Co., Inc., USA), absolute ethanol (99.9% pure) (Synth, Diadema, SP, Brazil), and hydrochloric acid (12 mol L^{-1}, Synth, Diadema, SP, Brazil) were used as received. Aqueous solutions were prepared using analytical-grade water from a Millipore Milli-Q Gradient filtration system.

2.2. Synthesis of nanoscale iron nanoparticles by green tea extract.

The synthesis of iron nanoparticles using green tea extracts was adapted from [3, 7, 13]. Briefly, the extract was prepared by heating 20 g L^{-1} green tea to 80°C. After settling for 1.0 h, the extract was filtered. The nanoparticles were obtained by using Fe^{2+}, Fe^{3+}, or a mixture of Fe^{2+}/Fe^{3+} solutions. Aqueous solutions of $FeCl_2.4H_2O$ (0.100 mol L^{-1}), $FeCl_3.6H_2O$ (0.100 mol L^{-1}) and a mixture of $FeCl_3.6H_2O$ (final concentration 0.05 mol L^{-1}) and $FeCl_2.4H_2O$ (final concentration of 0.100 mol L^{-1}) were prepared. A volume of 5.0 mL of each iron solution (Fe^{2+}, Fe^{3+}, or Fe^{2+}/Fe^{3+}) was separately added to 5.0 mL of green tea extract, followed by gentle mixing for 15 minutes. The formation of iron nanoparticles occurs immediately after the mixture of the green tea extract with solutions of Fe^{2+}, Fe^{3+}, or Fe^{2+}/Fe^{3+}, this is proven by the darkening of the suspension. After complete reduction, these mixtures were centrifuged at 10,000 rpm to separate out the solid nanomaterials, followed by ethanolic washing for further characterization.The obtained iron nanoparticles were dried prior the analysis.

2.3. Characterization of iron nanoparticles. Iron nanoparticles obtained from the reduction of Fe^{2+}, Fe^{3+} or Fe^{2+}/Fe^{3+} by green tea extract were characterized by different techniques, as described below.

2.3.1. X-ray diffraction (XRD).

X-ray diffractogram patterns of iron nanoparticles were obtained with approximately 200 mg powdered the nanomaterial deposited onto a glass substrate of 2 cm × 2 cm. The measurements were performed in reflection geometry with a conventional X-ray generator (CuKα radiation of 1.5418˚A and a graphite monochromator, Shimadzu XRD-700 diffractometer coupled to a scintillation detector). The samples were measured from 20°to 80° (2θ) with a step size of 0.05° and a counting time of 5 s per step.

2.3.2. Transmission electron microscopy (TEM).

Images of the iron nanoparticles were obtained by TEM (LIBRA 120, accelerating voltage of 120 kV; Zeiss International, Oberkochen, Germany) with an energy filtered transmission electron microscopy (electron energy loss spectroscopy, EELS detector). The distributions of iron (Fe) and carbon (C) atoms were mapped by the EELS technique. Prior analysis, nanoparticle samples were sonicated and mounted on 200 mesh holey carbon coated copper grids.

2.3.3. Scanning Electron Microscopy (SEM) and Energy Dispersive X-Ray Fluorescence Spectrometry (EDS).

Images of iron nanoparticles were obtained by SEM (Jeol JSM T-300 electron microscope Tokyo, Japan) at a voltage of20 KV, with an EDS system. The distributions of iron (Fe), oxygen (O), and sulfur (S) atoms on the surface of iron nanoparticles were mapped by the EDS technique.

2.3.4. Fourier transform infrared (FTIR) spectroscopy.

Iron nanoparticles were triturated with pure potassium bromide (KBr) powder. These mixtures were ground into fine powders, pressed in a mechanical press to generate translucent pellets and analyzed using a Bomen B-100 spectrometer. A pure KBr pellet was used for the background. The FTIR spectra were recorded from 400 to 4000 cm^{-1} at a resolution of 4 cm^{-1}.

2.3.5. Hydrodynamic size, size distribution and zeta potential.

The hydrodynamic diameter, polydispersity index (PDI) and zeta potential of iron nanoparticles were measured by dynamic light scattering (DLS) (Nano ZS Zetasizer, Malvern Instruments Corp.) at 25 °C in polystyrene cuvettes with a path length of 10 mm. The measurements were performed in triplicate with the standard error of the mean.

2.3.6. UV-Visible spectroscopy measurements.

UV-Visible spectra of 10-fold diluted green tea extract and iron nanoparticles aqueous suspension were recorded in a UV-Vis spectrophotometer (Agilent, model 8553, Palo Alto, CA, USA).

2.3.7. Quantification of free thiol groups on the surface of iron nanoparticles.

Free thiol (SH) groups on the surfaces of iron nanoparticles were quantified by titration with the 5,5`-dithiobis-(2-nitrobenzoic acid) (DTNB) reaction based on the absorbance at 412 nm(ε = 14,150 $mol^{-1}L^{1}cm^{-1}$) of the 2-nitro-5-thiobenzoate anion (TNB^{2-}) generated in the reaction of SH groups with DTNB [35, 36]. Briefly, 1.0 mg of iron nanoparticles was dispersed in 1.5 mL of water and added to 200 µL of DTNB (10 mmol L^{-1}) in PBS buffer (pH 7.4) containing 1.0 mmol $L^{-1}$of EDTA. After 5 min of incubation, the suspensions were centrifuged. The supernatant was placed into a quartz cuvette, and the absorption band at 412 nm was measured using a UV-Vis Spectrophotometer (Agilent, model 8553, Palo Alto, CA, USA). The experiments were performed in triplicate with the standard error of the mean.

2.3.8. Nitrosation of thiol groups of iron nanoparticles.

The nitrosation of free thiol groups on the surface of iron nanoparticles leading to the formation of S-nitroso-iron nanoparticles was performed as previous described [37, 38].

Briefly, iron nanoparticles were suspended in acidified deionized water (2.0 mg mL^{-1}, pH = 4.0). A volume of 200 µL of 60mmol L^{-1} of sodium nitrite in aqueous solution was added to the iron nanoparticles suspension. Molar excess of sodium nitrite related to the amount of thiol groups on the surface of iron nanoparticles was employed. After 30 min of incubation, the nanoparticle suspension was filtered by centrifugal ultrafiltration using a Microcon centrifugal filter device containing ultrafiltration membranes (MWCO 10-kDa molar mass cutoff filter, Millipore, Billerica, MA, USA) and washed five times with deionized water to remove excess of unreacted nitrite. This procedure led to the preparation of S-nitrosothiol groups on the surface of iron nanoparticles [38].

2.3.9. Quantification of NO release from S-nitroso- iron nanoparticles.

The amount of NO released from S-nitroso- iron nanoparticles was measured by the NO electrode (2.0 mm ISO-NOP) connected to a TBR4100/1025 Free Radical Analyzer (World Precision Instruments, Sarasota, FL, USA). Aliquots of 500 µL of aqueous suspensions S-nitroso-iron nanoparticles (2.0 mg mL^{-1}) were added to the sampling compartment, which contained 10 mL of an aqueous solution of copper(II) chloride ($CuCl_2$) (0.1 mol L^{-1}). This condition allowed for the detection of free NO released from the S-nitrosothiol groups present on the surface of the nanoparticle, as previous described [35]. Control groups were prepared by the addition of non-nitrosated iron nanoparticles, and sodium nitrite solution. The experiments were performed in duplicate with the standard error of the mean. Calibration curves were obtained with aqueous solutions of freshly prepared S-nitrosoglutathione (1 – 200 µmol L^{-1}) (data not shown).

3.RESULTS SECTION

3.1. Synthesis of iron nanoparticles by green tea extract.

Several reports described the successfully preparation of iron nanoparticles by biogenic routes, including plant extract as powerful reducing agents [5, 6, 15]. The great advantages of the use of plant extract in biogenic synthesis of metallic nanoparticles are the low-cost and simplicity, since the reduction reaction takes place at room temperature in a few minutes [15, 16, 20].

Among the plant extracts, green tea (*Camellia sinensis*) is the most used reducing agent of metal ions [15]. Green tea contains polyphenols, which act not only as reducing agents (reducing Fe^{2+} or Fe^{3+} to Fe^{0}), but also as capping agent. Indeed, the reduction of Fe^{2+} or Fe^{3+} to Fe^{0} by polyphenols occurs spontaneously, in which polyphenolsare oxidized to quinones [20].

It has been reported that this reduction takes places by the following steps: firstly, the complexation with Fe salts, the simultaneous reduction of Fe^{2+} or Fe^{3+}, and finally the capping of the obtained iron nanoparticles by molecules derived from the green tea extract, mainly polyphenols and caffeine [29]. Therefore, the presence of capping polyphenols on the surface of iron nanoparticles act as antioxidant and as scavenger of free radicals, allowing the storage of the nanoparticles for longer periods [20].

3.2. Characterization of iron nanoparticles synthesized by green tea extract.

In this work, iron nanoparticles were synthesized from the reduction of Fe^{2+}, Fe^{3+} or a mixture of Fe^{2+}/Fe^{3+} by green tea extract. The plant extract was proven to effectively reduce Fe^{2+}, Fe^{3+} or a mixture of Fe^{2+}/Fe^{3+} to iron nanoparticles. In order to avoid multiple Figures, for the most of the characterizations, data will present the results for the reduction of Fe^{3+} by green tea. It should be noted that similar results were observed for iron nanoparticles obtained from the reduction of Fe^{2+} or a mixture of Fe^{2+}/Fe^{3+}.

3.2.1. XRD analysis.

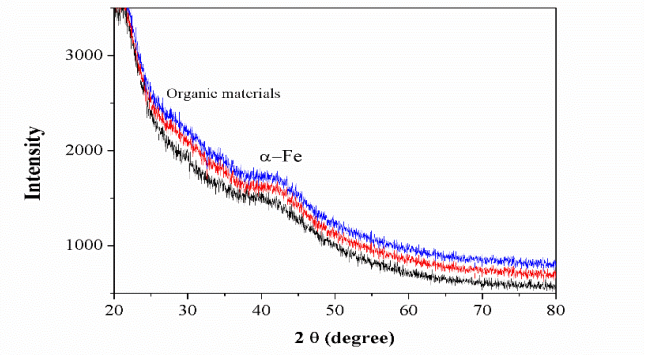

Figure 1. XRD patterns of iron nanoparticles synthesized by the reduction of Fe^{2+} (black line), Fe^{3+} (red line), and a mixture of Fe^{2+}/Fe^{3+} (blue line) by green tea extract.

Figure 1 shows the XRD patters of iron nanoparticles synthesized by the reduction of Fe^{2+} (black line), Fe^{3+} (red line), anda mixture of $Fe^{2}+/Fe^{3+}$ (blue line) by green tea extract.

In all cases (black, red and blue curves) it can be observed that the whole pattern is deficient in distinctive diffraction peaks, indicating that the obtained nanoparticles are mainly amorphous in nature [7]. As expected, a less obvious characteristic peak of iron nanoparticles (α-Fe) at *ca*. 2θ of 44.7° was found [9, 10, 14, 23, 29, 31]. Moreover, as indicated in Figure 1, the broad shoulder peak at *ca*. 27° can be assigned to the presence of organic materials adsorbed from the green tea extract as capping agent, as previously described for biogenic iron nanoparticles [3,23]. Very broad XDR peaks are reported for iron nanoparticle samples due to the short range order structure, which means the presence of amorphous nature of the iron nanophases, including the Fe(0) phase. Moreover, green routes are known to produce amorphous iron nanoparticle samples [1].

3.2.2. TEM and EELS analyses.

Figure 2 shows representative images of iron nanoparticles synthesized by the reduction of Fe^{3+} (Figure 2A,B) and a mixture of Fe^{2+}/Fe^{3+} (Figure 2C, D) by green tea extract.

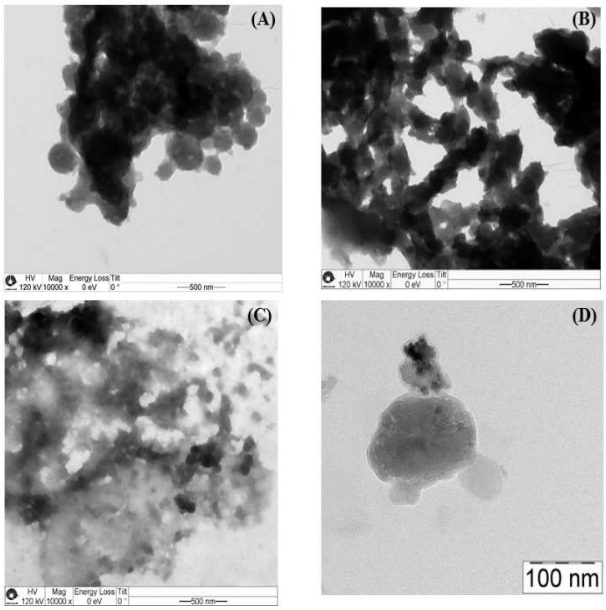

Figure 2. TEM images of iron nanoparticles synthesized by green tea extract: from the reduction of Fe^{3+} (A,B) and a mixture of Fe^{2+}/Fe^{3+} (C, D).

All synthesized iron nanoparticles appeared to be spherical in shape with varied size in the range of 10 to 200 nm, as previous described [7, 10, 22, 25, 30]. Moreover, the samples tend to organize in 2-D chain-line arrangements (Figure 2B), and the formation of cluster aggregates is observed. This tendency to agglomeration has already been described for iron nanoparticles synthesized by either chemical methods [30, 39], and biogenic routes [7, 10, 22, 25]. It should be noted that different sizes, shapes and levels of aggregations have been described for biogenic iron nanoparticles, as a result of the distinct antioxidants (polyphenols, caffeine, free amino acids, among others) present in each extract, which can react differently with the iron ions [7]. Hence, the chemical nature of the plant extract might interact with the iron nanoparticles by enhancing or hindering the nanoparticle growth, leading to different nanoparticle sizes and shapes [7]. Indeed, Nadagouda*et al*. [29] have reported the synthesis iron nanoparticles with different morphologies and shape by using tea extract.

Figure 3(A) shows a representative TEM image of iron nanoparticles obtained by the reduction of Fe^{3+} by green tea extract, and the corresponding mapping distributions of carbon atoms (Figure 3(B)), and iron atoms (Figure 3(C)), by EELS technique. The iron atoms are expected to be present in the nanoparticle core, and the carbon atoms, presented on the surface of the nanoparticles, are originated from the organic compounds of green tea extract, mainly polyphenols. Figure 3(D) shows the EELS scans of selected area of TEM image of the nanoparticle (Figure 3(C)). The peaks of 711 eV, 716 eV and 722 eV (Figure 3D) are assigned to $Fe2p_{3/2}$, shake-up satellite $2p_{3/2}$ and $2p_{1/2}$, respectively [30, 25, 40, 41]. These peaks suggested that the surface of iron nanoparticles consist of a layer of mixed oxides, mainly FeO, close to the Fe(0) interface [30, 40]. In addition, a discrete shoulder nearby 717 eV is resulted from the overlap of the shakeup satellite of oxidized iron ($2p_{3/2}$) and zero valent iron (Fe(0)) ($2p_{1/2}$) [10].

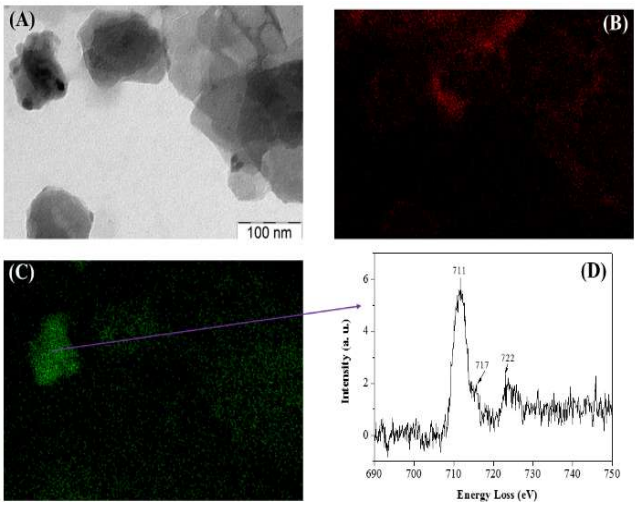

Figure 3. TEM image of iron nanoparticles synthesized by the reduction of Fe^{3+} by green tea extract (A), carbon atom mapping by EELS (B), iron atom mapping by EELS, (D) EELS spectrum of the arrow indicated area of nanoparticle in Figure. (3C).

3.2.3. SEM and EDS analyses.

Figure 4(A) shows a representative SEM image of iron nanoparticles synthesized by the reduction of Fe^{3+} by green tea extract. Nanoparticle agglomeration/aggregation can be observed. Indeed, SEM image reveals clustering of particles into sub-micron-scale aggregates. These structural features are in agreement with similarly prepared iron nanoparticles reported in the literature [2, 25, 42, 43]. The surface composition of Figure 4(A) was examined by EDS. Figure 4 shows the EDS elemental mapping of Fe atoms (Figure 4B), O atoms (Figure 4C), and S atoms (Figure 4D). As expected, iron is present in the core of the materials, and in lesser extend as capping agent, since green tea extract are known to content iron [44 - 46]. The presence of carbon (Figure 3B) and oxygen (Figure 4C) are attributed mainly to the polyphenol groups and other C, O-containing molecules in green tea extracts [23, 47, 48]. Nevertheless, the O signals may indicate the formation of some iron oxide nanoparticles as well, as demonstrated in Figure 3D. Moreover, the sulfur atom signal (Figure 4D) is due to the presence of sulfur in green tea extract, as previous reported [49].

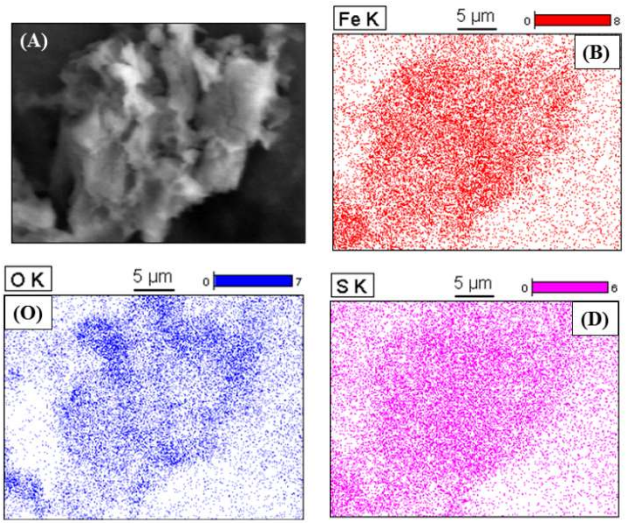

Figure 4. SEM image of the iron nanoparticles obtained by the reduction of Fe^{3+} by green tea extract (A), SEM image with EDS in which red dots corresponds to the mapping of iron atoms (B), oxygen atoms (O), and sulfur atoms (D).

3.2.4. FTIR analysis.

FTIR measurements were carried out to confirm possible composition of synthesized iron nanoparticles. Figure 5 shows the FTIR spectra of iron nanoparticles synthesized by the reduction of Fe^{2+} (black line), Fe^{3+} (red line), a mixture of Fe^{2}+/Fe^{3+} (blue line) by green tea extract.Figure 5 reveals similar FTIR profile for all curves, indicating the presence of the same capping agents on iron nanoparticle surfaces. The bands at 3420 cm^{-1} and 2924 cm^{-1} are associated with O-H stretching vibrations and C-H and CH_2 vibration of aliphatic hydrocarbons, respectively [10, 23, 27]. Bands at 1640 cm^{-1}, 1533 cm^{-1}, 1446 cm^{-1}, and 1370 cm^{-1} are associated with C-O-C, phenyl group, COO-, and C-N stretching vibration for aromatic amines, respectively, indicating the presence of water-soluble polyphenols and caffeine from the green extract [17, 23, 27, 50]. Band at 1040 cm^{-1} is associated with C-O-C stretching vibration [17, 23, 24]. Moreover, the bands at 613 cm^{-1} and 520 cm^{-1} are assigned to Fe-O [13], indicating the presence of oxidized iron oxide, which is consistent with the results obtained from EELS. Taken together, these results clearly demonstrated the presence of green tea polyphenols capped to the surface of iron nanoparticles.

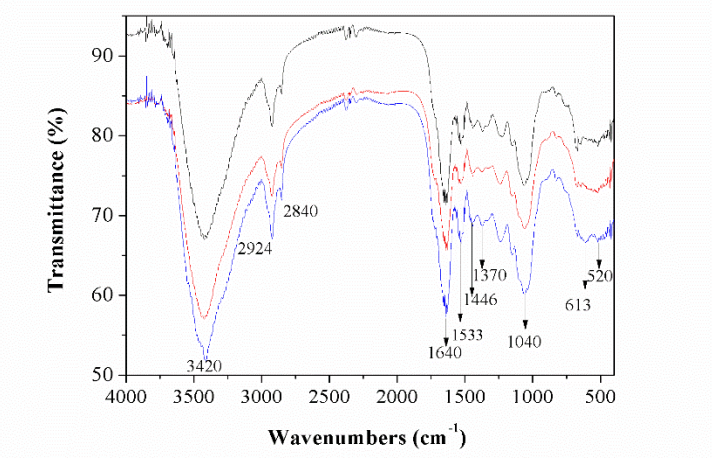

Figure 5.FTIR spectra of iron nanoparticles synthesized by the reduction of Fe^{2+} (black line), Fe^{3+} (red line), and Fe^{2+}/Fe^{3+} (blue line) by green tea extract.

3.2.5. Hydrodynamic size, size distribution and zeta potential.

DLS is a commonly technique to determine the size and aggregation behavior of nanoparticles in suspension [1]. The average hydrodynamic size of iron nanoparticles was found to be 53.7 ± 10.4 nm, and the polydispersity index (PDI) was 0.35 ± 0.02. These results indicates the formation of iron particles at the nanosize scale in aqueous suspension, and the PDI value suggests that the size distribution is moderate polydispersive. Our results are in accordance with the literature [1]. Figure 6 shows a representative size distribution of iron nanoparticles in aqueous suspension. A monomodal size distribution was observed, although there is a population of iron nanoparticles with hydrodynamic size over 100 nm.

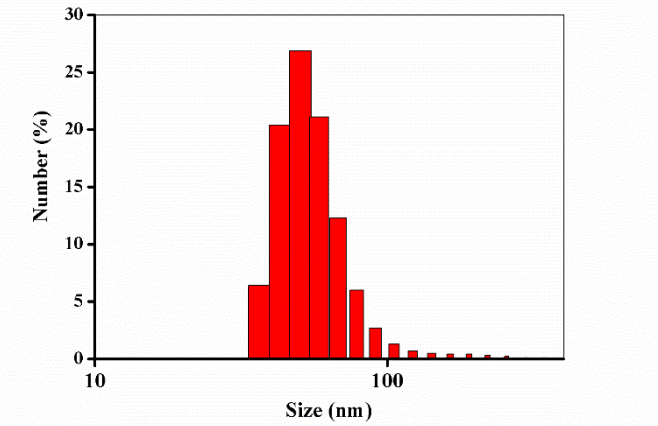

Figure 6. Representative particle size distribution for iron nanoparticles obtained from the reduction of Fe^{3+} by green tea extract, in aqueous suspension.

The zeta potential of iron nanoparticles was found to be – 23 ± 2.5 mV. As previous reported, negative value of zeta potential is expected for green tea polyphenol coated nanomaterials [51]. This negative charge is due to the presence of polyphenols/caffeine on the surface of the synthesized nanoparticles, which is responsible to minimize nanoparticle agglomeration.

3.2.6. UV-Visible spectroscopy measurements.

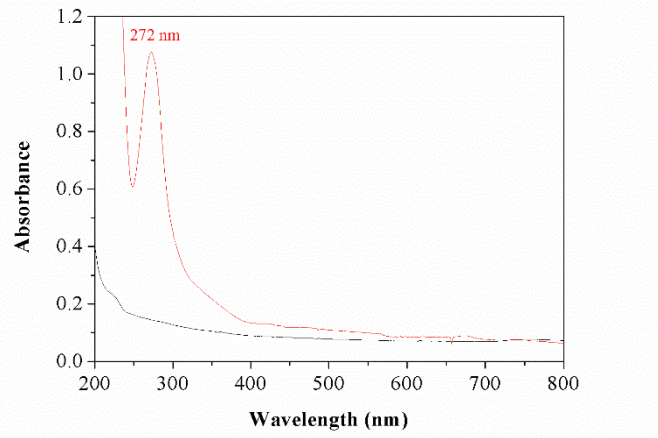

Figure 7. UV-visible spectra of iron nanoparticles (black line), and green tea extract (red line).

Figure 7 shows the UV-Visible spectrum of green tea extract (red line). The absorption peak at 272 nm is assigned to the presence of tea polyphenols and caffeine [13]. The formation of iron nanoparticles (Figure 7 black line) is characterized by the presence of UV spectrum with broad absorption, and there is no

sharp absorption bands, as can be observed the disappearance of the UV absorption band at 272 nm, as previous described [3]. Therefore, the formation of iron nanoparticles is suggested by the continuous absorption in the UV-Visible region, as already reported for biogenic synthesized iron nanoparticles using tea polyphenols [22, 29].

3.2.7. Quantification of free thiol groups on the surface of iron nanoparticles.

The quantification of free thiol (SH) groups on the surface iron nanoparticles was determined by the reaction with a thiol-specific reagent, DTNB [35]. Values of 45.5 ± 7.2 and 25.7 ± 4.5 µg mol of SH per gram of iron nanoparticles synthesized by the reduction of Fe^{3+} and a mixture of Fe^{2+}/Fe^{3+}, respectively, by green tea extract were obtained. These results is in accordance with the presence of sulfur atom on the surface of green tea synthesized iron nanoparticles, as demonstrated by EDS (Figure 4D). In drug delivery applications, the presence of free SH groups on the surface of nanoparticles represents a site for nanoparticle conjugation with important therapeutic molecules [33, 38]. Sulfur is one of the six major minerals found in green tea [45]. Indeed, the *Camellia sinensis* tea is the richest source of K, Cu, S and Al, as assayed by inductively coupled plasma optical emission spectrometry (ICP-OES) [49]. In addition, the presence of sulfur atoms on the surface of iron nanoparticles might be resulted from cysteine-containing amino acids and proteins found in green tea extract [52].

3.2.8. Nitrosation of thiol groups leading to the formation of S-nitroso-iron nanoparticles.

In the present study, thiol groups (SH) present on the surface of green tea synthesized iron nanoparticles were nitrosated by the addition of sodium nitrite in acidified solution, leading to the formation of S-nitroso-iron nanoparticles, which act as spontaneous NO donor (Figure 8). Acidified aqueous solution of nitrite (NO_2^-) is in equilibrium with nitrous acid (HNO_2) [35, 37, 38]. Nitrous acid is considered the nitrosating agent of SH groups yielding S-NO (S-nitroso) groups. S-NO groups act as spontaneous NO donor, due to the homolitic S-N bond cleavage with free NO release [35, 37, 38].

The quantification of NO release fromS-nitroso-iron nanoparticles was performed by electrochemical analysis with a specific NO sensor. Values of 42.9 ± 5.1 and 22.2 ± 5.1 µg mol of NO per gram of iron nanoparticles synthesized by the reduction of Fe^{3+} and a mixture of Fe^{2+}/Fe^{3+}, respectively, by green tea extract were obtained.

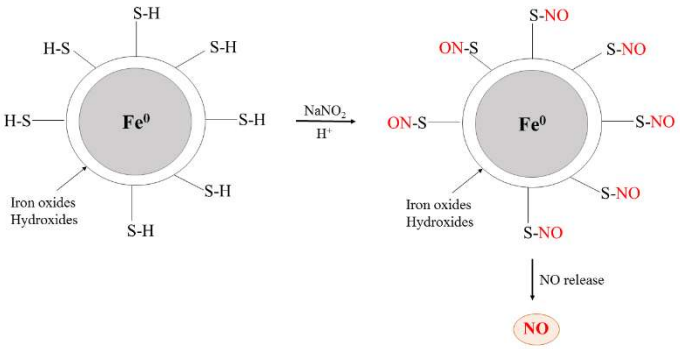

Figure 8. Schematic representation of the nitrosation of thiol groups on the surface of green tea synthesized iron nanoparticles by the addition of acidified aqueous sodium nitrite, leading to the formation of S-nitroso-iron nanoparticles, which are spontaneous NO donor.

This amount of NO release from S-nitroso-iron nanoparticles is a similar range of the amount of NO release from S-nitroso-iron oxide magnetic nanoparticles, as reported by Molina *et al*. [37] and Santos *et al*. [35]. It should be noted that this amount of NO release from S-nitroso-iron nanoparticles (in the range of µmol of NO per gram of nanoparticle) might find important biomedical applications, such as the promotion of wound healing process, increase of blood flow, and platelet adhesion inhibition [53]. Therefore, green tea synthesized iron nanoparticles can be successfully nitrosated, leading to the formation of S-nitroso-iron nanoparticles, which release therapeutic amounts of NO that can be use in different biomedical applications. To our best knowledge, this is the first report that describes the formation of S-nitroso groups on the surface of biogenic synthesized iron nanoparticles. Administration of exogenous sources of NO donors, such as NO-releasing nanoparticles might find important biomedical applications including the cytotoxicity towards cancer cell lines and invading parasites, the promotion and acceleration of wound repair process, the promotion of blood vessel dilation and the inhibition of platelet adhesion and aggregation [33, 53, 54].

4. CONCLUSIONS

This study describes the biogenic synthesis of iron nanoparticles by green tea extract. Characterization of the as-synthesized iron nanoparticles revealed that the nanoparticles have spherical shape, and cluster aggregation was observed. The surface of iron core consisted of a layer of mixed oxide. The average hydrodynamic size of the nanoparticles was found to be 53.7 ± 10.4 nm, as assayed by dynamic light scattering. As expected, green tea polyphenols capped the surface of iron nanoparticles. Free thiol groups on the surface of green tea synthesized iron nanoparticles was nitrosated by the generation of nitrous acid from acidified nitrite solution. The amount of NO release from S-nitroso-iron nanoparticles was found to be in the low micro mol of NO per gram of nanoparticles. These results highlight that S-nitroso-iron nanoparticles might find important biomedical applications as engineered biogenic nanomaterial to carry and delivery therapeutic amounts of NO in diverse pharmacological applications. Toxicological evaluations of NO-releasing biogenic iron nanoparticles are currently in progress.

5. REFERENCES

[1] Chekli L., Bayatsarmadi B., Sekine R., Sarkar B., Maoz Shen A., Scheckel K.G., Skinner W., Naidu R., Shon H.K., Lombi E., Donner E., Analytical characterization of nanoscale zero-valent iron: A methodological review, *Anal. Chim. Acta*, 903, 13-35, **2016.**

[2] Han Y., Yang M.D.Y., Zhang W., Yan W., Optimizing synthesis conditions of nanoscale zero-valent iron (nZVI) through aqueous reactivity assessment, *Front. Environ. Sci. Eng*., 9, 5, 813–822, **2015.**

[3] Hoag G.E., Collins J.B., Holcomb J.L., Hoag J.R., Nadagouda M.N., Varma R.S., Degradation of bromothymol blue by 'greener' nano-scale zero-valent iron synthesized using tea polyphenols, *J, Mater, Chem*., 19, 8671–8677, **2009.**
[4] Noubactep C., Metallic iron for environmental remediation: A review of reviews, *Water Res*., 85, 114-123, **2015.**
[5] Stefaniuk M., Oleszczuk P., Ok Y.S., Review on nanozerovalent iron (nZVI): From synthesis to environmental applications, *Chem, Eng, J*., 287, 618-632, **2016.**
[6] Kharisov B.I., Dias H.V.R., Kharissova O.V., Jiménez-Pérez V.M., Pérez B.O., Flores B.M., Iron-containing nanomaterials: synthesis, properties, and environmental applications, *RSC Advances*, 2, 9325–9358, **2012.**
[7] Machado S., Pacheco J.G., Nouws H.P.A., Albergaria J.T., Delerue-Matos C., Characterization of green zero-valent iron nanoparticles produced with tree leaf extracts, *Sci, Total Environ*., 533, 76-81, **2015.**
[8] Ou Y.-H., Wei C.-Y., Shih Y.-H., Short-chain organic acids increase the reactivity of zerovalent iron nanoparticles toward polychlorinated aromatic pollutants, *Chem. Eng. J*., 284, 372-379, **2016.**
[9] Wang X., Wang P., Liu H., Ning P., Synthesis, characterization, and reactivity of cellulose modified nanozero-valent iron for dye discoloration, *Appl. Surf. Sci*., 345, 57-66, **2015.**
[10] Xiao J., Gao B., Yue Q., Gao Y., Li Q., Removal of trihalomethanes from reclaimed-water by original and modified nanoscale zero-valent iron: Characterization, kinetics and mechanism, *Chem. Eng. J*., 262, 1226-1236, **2015.**
[11] Zha S., Cheng Y., Gao Y., Chen Z., Megharaj M., Naidu R., Nanoscale zero-valent iron as a catalyst for heterogeneous Fenton oxidation of amoxicillin, *Chem. Eng. J*., 255, 141–148, **2014.**
[12] Goldstein N., Greenlee L.F., Influence of synthesis parameters on iron nanoparticle size and zeta potential, *J. Nanopart. Res*., 14, 760, **2012.**
[13] Huang D.-L., Chen G.-M., Zeng G.-M., Xu P., Yan M., Lai C., Zhang C., Li N.-J., Cheng M., He X.-X., He Y., Synthesis and application of modified zero-valent iron nanoparticles for removal of hexavalent chromium from wastewater, *Water Air Soil Pollut*., 226, 375, **2015.**
[14] Jamei M.R., Khosravi M.R., Anvaripour B., A novel ultrasound assisted method in synthesis of NZVI particles, *Ultrason. Sonochem*., 21, 226-233, **2014.**
[15] Herlekar M., Barve S., Kumar R., Plant-mediated green synthesis of iron nanoparticles, *J. Nanopart. Res.,* Article ID 140614, **2014.**
[16] Seabra A.B., Durán N., Nanotoxicology of metal oxide nanoparticles, *Metals* 5, 2, 934-975, **2015.**
[17] Huang L., Luo F., Chen Z., Megharaj M., Naidu R., Green synthesized conditions impacting on the reactivity of Fe NPs for the degradation of malachite green, *Spectrochim. Acta A*, 137, 154–159, **2015.**
[18] Rubilar O., Rai M., Tortella G., Diez M.C., Seabra A.B., Durán N., Biogenic nanoparticles: copper, copper oxides, copper sulphides, complex copper nanostructures and their applications, *Biotechnol. Lett*., 35, 9, 1365-1375, **2013.**
[19] Seabra A.B., Durán N., Metallic oxide nanoparticles: state of the art in biogenic syntheses and their mechanisms, *Appl. Microbiol. Biotechno*l., 95, 2, 275-288, **2012.**
[20] Seabra A.B., Haddad P.S., Durán N., Biogenic synthesis of nanostructured iron compounds: applications and perspectives, *IET Nanobiotechnol*., 7, 3, 90-99, **2013.**
[21] de Lima R., Seabra A.B., Durán N., Silver nanoparticles: a brief review of cytotoxicity and genotoxicity of chemically and biogenically synthesized nanoparticles, *J. Appl. Toxicol*., 32, 11, 867-879, **2012.**
[22] Njagi E.C., Huang H., Stafford L., Genuino H., Galindo H.M., Collins J.B., Hoag G.E., Suib S.L., Biosynthesis of iron and silver nanoparticles at room temperature using aqueous sorghum bran extracts, *Langmuir*, 27, 1, 264–271, **2011.**
[23] Wang T., Jin X., Chen Z., Megharaj M., Naidu R., Green synthesis of Fe nanoparticles using eucalyptus leaf extracts for treatment of eutrophic wastewater, *Sci. Total Environ*., 466–467, 210–213, **2014.**
[24] Weng X., Huang L., Chen Z., Megharaj M., Naidu R., Synthesis of iron-based nanoparticles by green tea extract and their degradation of malachite, *Ind. Crop. Prod*., 51, 342– 347, **2013.**
[25] Shahwan T., Sirriah S.A., Nairat M., Boyaci E., Eroglu A.E., Scott T.B., Hallam K.R., Green synthesis of iron nanoparticles and their application as a Fenton-like catalyst for the degradation of aqueous cationic and anionic dyes, *Chem. Eng. J*., 172, 258-266, **2011.**
[26] Kuang Y., Wang Q., Chen Z., Megharaj M., Naidu R., Heterogeneous Fenton-like oxidation of monochlorobenzene using green synthesis of iron nanoparticles, *J. Colloid Interface Sci*., 410, 67-73, **2013.**
[27] Kumar K.M., Mandal B.K., Kumar K.S., Reddy P.S., Sreedhar B., Biobased green method to synthesize palladium and iron nanoparticles using *Terminalia chebula* aqueous extract, *Spectrochim. Acta A*, 102, 128-133, **2013.**
[28] Pattanayak M., Nayak P.L., Ecofriendly green synthesis of iron nanoparticles from various plants and spices extract, *Int. J. Pl. An. and Env. Sci*., 3, 1, 68-78, **2013.**
[29] Nadagouda M.N., Castle A.B., Murdock R.C., Hussainb S.M., Varma R.S., *In vitro* biocompatibility of nanoscale zerovalent iron particles (NZVI) synthesized using tea polyphenols, *Green Chem*., 12, 114–122, **2010.**
[30] Cirtiu C.M., Raychoudhury T., Ghoshal S., Moores A., Systematic comparison of the size, surface characteristics and colloidal stability of zero valent iron nanoparticles pre- and post-grafted with common polymers, *Colloids Surf. A*, 390, 95– 104, **2011.**
[31] Jin X., Zhuang Z., Yu B., Chen X., Chen Z., Functional chitosan-stabilized nanoscale zero-valent iron used toremove acid fuchsine with the assistance of ultrasound, *Carbohyd. Polym.*, 136, 1085–1090, **2016.**
[32] Seabra A.B., Marcato P.D., de Paula L.B., Durán N., New strategy for controlled release of nitric oxide, *J. Nano Res*., 20, 61-67, **2012.**
[33] Seabra A.B., Justo G.Z., Haddad P.S., State of the art, challenges and perspectives in the design of nitric oxide-releasing polymeric nanomaterials for biomedical applications, *Biotechnol. Adv*., 33, 1370-1379, **2015.**
[34] Seabra A.B., Durán N., Nitric oxide-releasing vehicles for biomedical applications, *J. Mater. Chem*., 20, 1624-1637, **2010.**
[35] Santos M.C., Seabra A.B., Pelegrino M.T., Haddad P.S., Synthesis, characterization and cytotoxicity of glutathione- and PEG-glutathione-superparamagnetic iron oxide nanoparticles for nitric oxide delivery, *Appl. Surf. Sci*., 367, 26–35, **2016.**
[36] Seabra A.B., Martins D., Simões M.M.S.G., da Silva R., Brocchi M., de Oliveira M.G., Antibacterial nitric oxide-releasing polyester for the coating of blood-contacting artificial materials, *Artif. Organs*, 34, 7, E204-E214, **2010.**
[37] Molina M.M., Seabra A.B., de Oliveira M.G., Itri R., Haddad P.S., Nitric oxide donor superparamagnetic iron oxide nanoparticles, *Mater. Sci. Eng. C Mater. Biol*., 33, 746-751, **2013.**
[38] Seabra A.B., Pasquoto T., Ferrarini A.C.F., Santos M.D., Haddad P.S., de Lima R., Preparation, characterization, cytotoxicity, and genotoxicity evaluations of thiolated- and S-nitrosated superparamagnetic iron oxide nanoparticles:

implications for cancer treatment, *Chem. Res. Toxicol*., 27, 1207-1218, **2014.**
[39] Sun Y.-P., Li X.-Q., Zhang W.-X., Wang H.P., A method for the preparation of stable dispersion of zero-valent iron nanoparticles, *Colloids Surf. A*, 308, 60–66, **2007.**
[40] Liu A., Zhang W.-X., Fine structural features of nanoscale zero-valent iron characterized by spherical aberration corrected scanning transmission electron microscopy (Cs-STEM), *Analyst,* 139, 4512–4518, **2014.**
[41] Wang Q., Kanel S.R., Park H., Ryu A., Choi H., Controllable synthesis, characterization, and magnetic properties of nanoscale zerovalent iron with specific high Brunauer–Emmett–Teller surface area, *J. Nanopart. Res*., 11, 749–755, **2009.**
[42] Martin J.E., Herzing A.A., Yan W., Li X.Q., Koel B.E., Kiely C.J., Zhang W.X., Determination of the oxide layer thickness in core-shell zerovalent iron nanoparticles, *Langmuir*, 24, 8, 4329–4334, **2008.**
[43] Nurmi J.T., Tratnyek P.G., Sarathy V., Baer D.R., Amonette J.E., Pecher K., Wang C., Linehan J.C., Matson D.W., Penn R.L., Driessen M.D., Characterization and properties of metallic iron nanoparticles: spectroscopy, electrochemistry, and kinetics, *Environ. Sci. Technol*., 39, 1221–1230, **2005.**
[44] Molan A.L., Flanagan J., Wei W., Moughan P.J., Selenium-containing green tea has higher antioxidant and prebiotic activities than regular green tea, *Food Chem*., 114, 829-835, **2009.**
[45] Ramdani D., Chaudhry A.S., Seal C.J., Chemical composition, plant secondary metabolites, and minerals of green and black teas and the effect of different tea-to-water ratios during their extraction on the ccomposition of their spent leaves as potential additives for ruminants, *J. Agric. Food Chem*., 61, 4961−4967, **2013.**
[46] Xu Y.-Q., Chen S.-Q., Shen D.-Y., Yin J.-F., Effects of chemical components on the amount of green tea cream, *Agr. Sci. China*, 10, 6, 969-974, **2011.**
[47] Lee L.S., Kim S.H., Kim Y.B., Kim Y.C., Quantitative analysis of major constituents in green tea with different plucking periods and their antioxidant activity, *Molecules*, 19, 7, 9173-9186, **2014.**
[48] Saldanha L., Dwyer J., Andrews K., Betz J., Harnly J., Pehrsson P., Rimmer C., Savarala S., Feasibility of including green tea products for an analytically verified dietary supplement database, *J. Food Sci*., 80, 4, H883-H888, **2015.**
[49] Olivier J., Symington E.A., Jonker C.Z., Rampedi I.T., van Eeden T.S., Comparison of the mineral composition of leaves and infusions of traditional and herbal teas, *S. Afr. J. Sci*., 108, ½, Article number 623, **2012.**
[50] Rakhshaee R., Decreasing Fe^0 and Fe_3O_4nano particle size by simultaneous synthesis on a bio-polymeric structure: Kinetic study to remove Amaranth from aqueous solution, *Powder Technol*., 254, 494–499, **2014.**
[51] Abdullah M.F., Zakaria R., Zein S.H.S., Green tea polyphenol–reduced graphene oxide: derivatisation, reduction efficiency, reduction mechanism and cytotoxicity, *RSC Adv*., 4, 34510–34518, **2014.**
[52] Yin J.-F., Xu Y.-Q., Yuan H.-B., Luo L.-X., Qian X.-J., Cream formation and main chemical components of green tea infusions processed from different parts of new shoots, *Food Chem*., 114, 665–670, **2009.**
[53] Ignarro L.J., Nitric oxide: biology and pathobiology, 1st ed. San Diego: Academic Press, **2000.**
[54] Georgii J.L., Amadeu T.P., Seabra A.B., de Oliveira M.G., Monte-Alto-Costa A., Topical S-nitrosoglutathione-releasing hydrogel improves healing of rat ischaemic wounds, *J. Tissue Eng. Regen. Med*., 5, 8, 612-619, **2011.**

6. ACKNOWLEDGEMENTS

This work was supported by FAPESP, the Brazilian Network on Nanotoxicology (MCTI/CNPq), the Laboratory of Nanostructure Synthesis and Biosystem Interactions-NANOBIOSS and INCT/INOMAT (Instituto Nacional de Ciência, Tecnologia & Inovaçãoem Materiais Complexos Funcionais).